Supporting Information

Cheng et al. 10.1073/pnas.1202435109

SI Materials and Methods

Metabolic Characterization of APPL1 Transgenic (Tg) and Knockout Mice (KO). The mice were fed either with a standard chow (STC) (Purina) with 20 kcal percentage of protein, 10 kcal percentage of fat, and 70 kcal percentage of combined simple carbohydrates or with a high-fat diet (HFD) (Research Diets) composed of 20 kcal percentage of protein, 45 kcal percentage of fat, and 35 kcal percentage of carbohydrates. Glucose tolerance test (GTT) was performed as described previously (1) in overnight-fasted mice after i.p. injection of D-glucose (2 g/kg). For insulin tolerance test (ITT), mice fasted for 6 h were intraperitoneally injected with human recombinant insulin (Novo Nordisk). To evaluate insulin secretion in vivo, overnight-fasted mice were intraperitoneally injected with 2 g/kg D-glucose or 1 g/kg L-arginine. Blood samples were taken from the tail vein for the measurement of glucose and insulin levels using a glucose meter and insulin ELISA kits (Antibody and Immunoassay Services, The University of Hong Kong), respectively.

Quantitative Real-Time PCR. Total RNA was extracted from isolated islets or INS-1E cells using TRIzol reagent (Invitrogen), and cDNA was synthesized from 0.5 μg total RNA by reverse transcription using an ImProm-II reverse transcription kit (Promega) with random hexamer primers. Quantitative real-time PCR was performed using SYBR Green QPCR system (Qiagen) with specific primers (Table S2). The PCR reactions were performed using an Applied Biosystems Prism 7000 sequence detection system. The level of target gene expression was normalized against the GAPDH gene.

Adenovirus Infection. Adenovirus encoding APPL1, luciferase control, scrambled control RNAi, and APPL1 RNAi were generated and purified as previously described (1). Adenovirus expressing the constitutively active form of Akt was a kind gift from Christopher J. Rhodes (University of Washington) (2). Isolated islets with similar size were selected and cultured overnight for adenovirus infection. Approximately 100 islets were infected with the adenovirus for 3 h at 37 °C at 100 multiplicity of infection (MOI), assuming 1,000 cells per islet on average, followed by incubation with the fresh medium for 36 h. INS-1E cells were infected with the adenovirus at 50 MOI and cultured as above.

Coimmunoprecipitation. INS-1E cells were infected with adenovirus encoding APPL1 RNAi or scrambled control for 40 h, followed by serum starvation for 6 h, and treated with insulin (50 nM) for 10 min. The cells were lysed in a mammalian cell lysis buffer [20 mM Tris-HCl, 150 mM NaCl, 1 mM Na_2EDTA, 1 mM EGTA, 1% Triton, 1 mM NaF, 1 mM Na_3VO_4 and protease inhibitor mixture (Roche), pH 7.4]. The total cell lysate was clarified by centrifugation at 20,000 × *g* for 15 min at 4 °C. Protein concentration was determined with BCA protein assay (Pierce Biotechnology). Five hundred micrograms of total protein was precleared by incubation with protein G agarose (Sigma) for 1 h at 4 °C. The precleared lysate was incubated with 2.5 μg of anti-Akt antibody at 4 °C overnight, followed by incubation with 10 μL protein G agarose for 1 h. The immunoprecipitated complex was eluted by boiling with 2× SDS/PAGE loading buffer at 99 °C for 5 min. The eluted samples were subjected to Western blot analysis.

Islet Isolation and Insulin Secretion Assay. Mice were fasted for 4 h and killed by cervical dislocation. Pancreas was perifused with collagenase P and subsequently digested at 37 °C for 20 min and then filtered through 500-μm and 70-μm cell strainers, resulting in two fractions: flow-through fraction containing exocrine cells (nonislet fraction) and captured fraction (islets). Captured islets were then picked manually under a microscope and maintained in RPMI 1640 culture medium supplemented with 10% (vol/vol) FBS at 37 °C overnight. The isolated islets or pancreatic β cells were washed twice with Krebs Ringer bicarbonate (KRB) buffer containing 0.1% fatty acid-free BSA supplemented with 3 mM glucose for 1 h, followed by stimulation with different stimulants for various time periods. For perifusion experiment, the isolated islets were incubated in KRB buffer for 30 min and perifused in KRB buffer containing 3 mM glucose for 6 min, and the perfusate was then switched to KRB buffer containing various concentrations of glucose. Eluted fractions were collected at 3-min intervals for 36 min. Insulin secreted in each fraction was measured using an insulin ELISA kit (Antibody and Immunoassay Services, The University of Hong Kong), and normalized for the number of islets or total amount of protein.

Histological, Immunohistochemical, and Electron Microscopic Analysis. Pancreases were isolated from mice, fixed in 4% paraformaldehyde in 0.1 M phosphate buffer, embedded in paraffin, and cut into 5-μm thick sections at 50-μm intervals. To determine the distribution of APPL1 in pancreas, pancreas sections of lean mice, diet-induced obese mice, and db/db diabetic mice were stained with rabbit anti-APPL1 (3) and mouse antiinsulin (HyTest) antibodies, followed by staining with secondary FITC-antirabbit IgG- and Cy3-antimouse IgG-conjugated antibodies, respectively. The pancreas section from APPL1 KO was used as a negative control. For the measurement of β-cell mass, pancreatic sections were stained with antiinsulin antibody, and the areas of β cells were quantified using an image analysis software (ImageJ 1.43U). The β-cell mass was evaluated by multiplying the pancreas weight by the percentage of β cells as described (4).

Electron microscopic analysis was performed by the Electron Microscope Unit at The University of Hong Kong. Briefly, isolated islets were fixed in 2.5% glutaraldehyde in cacodylate, osmicated in 1% osmium tetroxide, dehydrated and infiltrated, and polymerized in epoxy resin. Sections of 100-nm thickness were prepared from the embedded samples. The thin sections were mounted on 150 mesh hexagonal copper grids, stained with 2% aqueous uranyl acetate and Reynold's lead citrate, and visualized on a Philips EM208s transmission electron microscope. Docked insulin granules were quantified as described previously (5).

Measurement of ATP Production and Calcium Influx. ATP level in the islets was measured with Luminescence ATP detection assay system (PerkinElmer). For calcium measurement, Fura-2 calcium indicator (molecular probe) was loaded onto isolated islet at 37 °C for 30 min, followed by washing with KRB buffer. Ratio of 340/380 was monitored using a calcium ion sensing system according to the manufacturer's instructions (IonOptix).

Two-Photon Excitation Imaging. The fusion pore dynamics and exocytosis of insulin granules in pancreatic islets were examined using two-photon excitation imaging as described (6). Briefly, pancreatic islets isolated from either 16-wk-old male APPL1 KO mice or WT controls were immersed in a solution containing 140 mM NaCl, 5 mM KCl, 2 mM $CaCl_2$, 1 mM $MgCl_2$, 10 mM Hepes (pH 7.4), and 3 mM glucose. The polar red fluorescent tracer sulforhodamine B (SRB; 0.7 mM) and/or 10-kDa fluores-

cein-dextran (1 mM) was added 10 min before stimulation with 20 mM glucose. Two-photon excitation imaging was performed with an upright microscope (LSM710; Carl Zeiss) equipped with a water immersion objective lens (W Plan-Apochromat 20×/1.0 DIC M27 75 mm; Carl Zeiss), and a laser-scanning microscope. Images were acquired every 0.5 s. Exocytotic events in response to glucose stimulation during the first 5 min were measured within an arbitrary area (1,000 μm^2) of islets. The fusion pore dynamics were examined by measuring latency of the onset of staining with SRB (1.4 nm) relative to that of staining with 10 kDa dextran (6 nm).

Statistical Analysis. Data are presented as mean ± SEM. All experiments were repeated three times with representative data shown. Statistical significance was determined by Student's two-tailed *t* test. A *P* value of less than 0.05 represented a significant difference in all statistical comparisons.

1. Cheng KK, et al. (2009) APPL1 potentiates insulin-mediated inhibition of hepatic glucose production and alleviates diabetes via Akt activation in mice. *Cell Metab* 9:417–427.
2. Dickson LM, et al. (2001) Differential activation of protein kinase B and p70(S6)K by glucose and insulin-like growth factor 1 in pancreatic beta-cells (INS-1). *J Biol Chem* 276:21110–21120.
3. Cheng KK, et al. (2007) Adiponectin-induced endothelial nitric oxide synthase activation and nitric oxide production are mediated by APPL1 in endothelial cells. *Diabetes* 56:1387–1394.
4. Okada T, et al. (2007) Insulin receptors in beta-cells are critical for islet compensatory growth response to insulin resistance. *Proc Natl Acad Sci USA* 104:8977–8982.
5. Straub SG, Shanmugam G, Sharp GW (2004) Stimulation of insulin release by glucose is associated with an increase in the number of docked granules in the beta-cells of rat pancreatic islets. *Diabetes* 53:3179–3183.
6. Takahashi N, Kishimoto T, Nemoto T, Kadowaki T, Kasai H (2002) Fusion pore dynamics and insulin granule exocytosis in the pancreatic islet. *Science* 297:1349–1352.

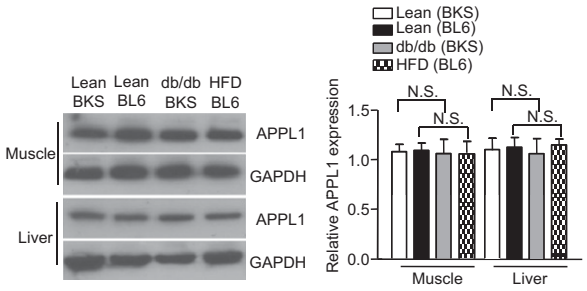

Fig. S1. Comparison of APPL1 expression levels in liver and skeletal muscle in healthy mice and obese/diabetic mice. Liver and soleus muscle were collected from 12-wk-old C57BKS db/+ lean mice, C57BKS db/db obese/diabetic mice, C57BL/6J lean mice, or HFD-induced obese mice for Western blot analysis as specified. *n* = 5. NS, not significant.

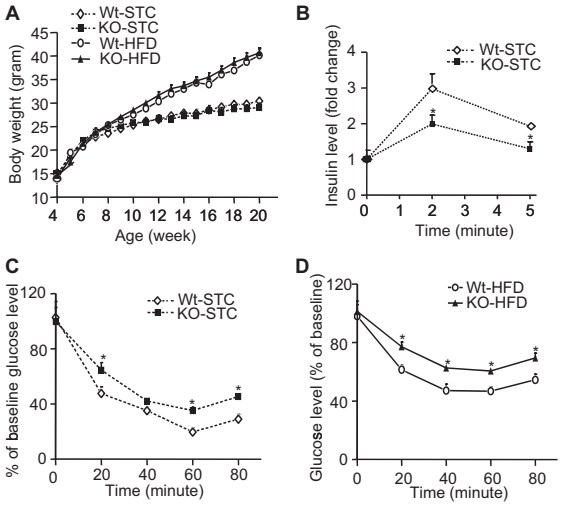

Fig. S2. Effects of APPL1 deficiency on body weight, insulin secretion, and insulin sensitivity in mice. (*A*) Body weights of male APPL1 KO mice and WT littermates fed with STC or HFD were measured weekly. (*B*) Serum insulin levels measured at various time points after L-arginine stimulation in 16-wk-old male mice fed with STC (fold change over basal insulin level). (*C* and *D*) Insulin tolerance test in 16-wk-old male APPL1 KO and WT littermates fed with STC or HFD, respectively. Data are expressed as percentage of baseline blood glucose values. **P* < 0.05 (*n* = 7).

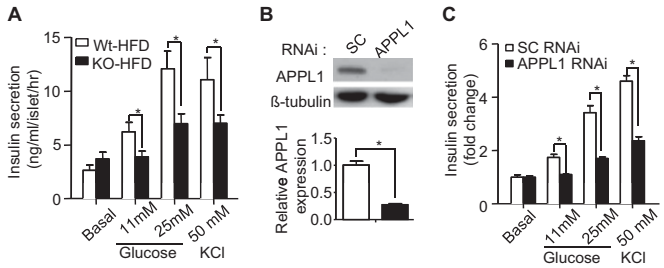

Fig. S3. APPL1 deficiency causes defective insulin secretion in both mouse islets and rat INS-1E β cells. (*A*) Glucose and KCl-stimulated static insulin secretion in islets isolated from 20-wk-old male APPL1 KO mice and WT controls on HFD. (*B*) Western blot analysis of APPL1 in INS-1E cells infected with adenovirus encoding scrambled control (SC) or APPL1 RNAi for 48 h (multiplicity of infection = 50 per cell). (*C*) Static insulin secretion in infected INS-1E cells measured after stimulation with glucose or KCl for 30 min (fold change over baseline). $*P < 0.05$ ($n = 4$).

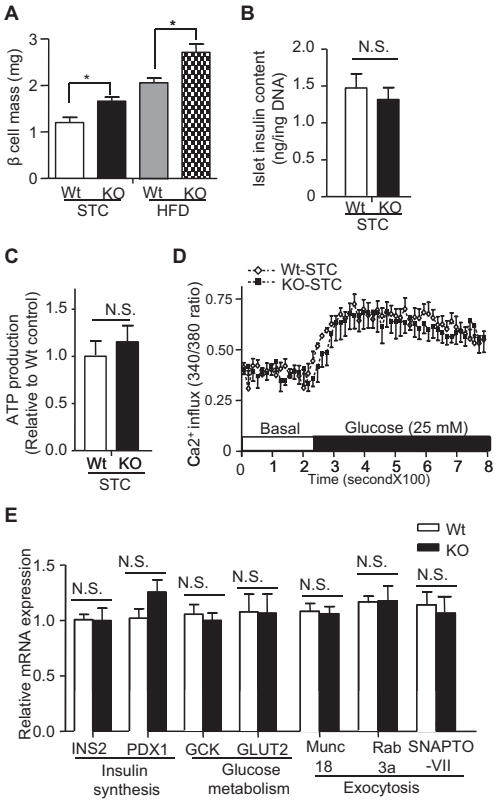

Fig. S4. Effect of genetic disruption of APPL1 on total insulin content, ATP production, calcium influx and expression of genes involved in insulin synthesis, glucose metabolism, and exocytosis in pancreatic islets. Islets isolated from 20-wk-old male APPL1 KO mice and WT littermates were used for the analysis. (*A*) Pancreatic β-cell mass. (*B*) Total insulin content in pancreatic islets expressed as nanogram of insulin per nanogram of DNA. (*C* and *D*) Intracellular ATP and calcium levels measured at 10 min after stimulation with glucose (25 mM), respectively. Note that calcium influx in isolated islets loaded with Fura-2 calcium indicator was determined by the ratio of 340/380 using the IonOptix system. (*E*) Real-time PCR analysis for mRNA expression of several key genes involved in insulin synthesis, glucose metabolism, and exocytosis. INS2, Insulin-2; PDX-1, pancreatic and duodenal homeobox 1; GCK, glucose kinase; GLUT2, glucose transporter 2; Munc18, Sec1/Munc18; SNAPTO-VII, synaptotagmin VII; NS, not significant. $n = 6$.

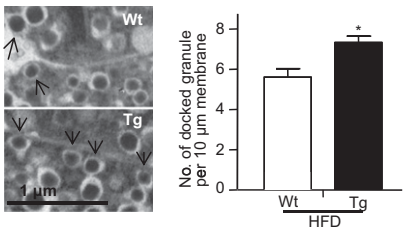

Fig. S5. Increased docking insulin granules in pancreatic islets of APPL1 transgenic mice. Islets were isolated from 20-wk-old male APPL1 Tg or WT mice fed with HFD and subjected to electron microscopic analysis. Representative electron microscopic images (*Left*) of docked insulin granules (denoted with arrows) and quantification of the number of docked granules (*Right*) in the islets. $P < 0.05$ ($n = 4$).

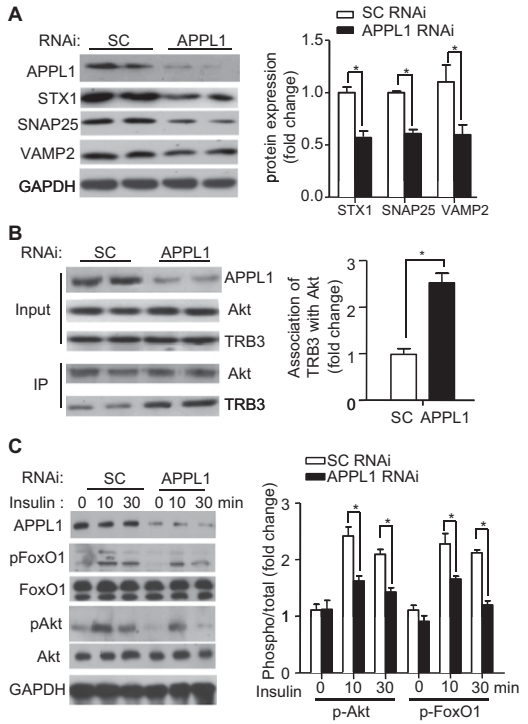

Fig. S6. Knockdown of APPL1 expression reduces the expression of SNARE proteins, enhances the interaction between Akt and TRB3, and inhibits insulin-induced Akt/FoxO1 phosphorylation in INS-1E cells. INS-1E cells were infected with adenovirus encoding APPL1 or scrambled control (SC) RNAi for 40 h, followed by starvation in a serum-free medium for 8 h. (*A*) Western blot analysis for the three SNARE proteins in the cell lysates (*Left*) and densitometric quantification for relative abundance of the three SNARE proteins (*Right*). (*B*) Total protein lysates from cells infected with adenovirus encoding APPL1 or SC RNAi were subjected to immunoprecipitation with a polyclonal antibody against Akt, followed by Western blot analysis with antibodies against Akt, APPL1, or TRB3 as indicated. Bar chart on the *Right* represents the relative fold change of association between Akt and TRB3 as quantified by densitometry. IP, immunoprecipitated complexes; input, total protein lysates. (*C*) Cells were treated with insulin (50 nM) for various periods as indicated and collected for Western blot analysis using antitotal or phospho-FoxO1 (Ser-256), antitotal or phospho-Akt (Ser-473), anti-APPL1, or anti-GAPDH antibody as a loading control. Bar chart on the *Right* represents the relative fold change of phosphorylation versus total as quantified by densitometry. $*P < 0.05$ ($n = 5$–6).

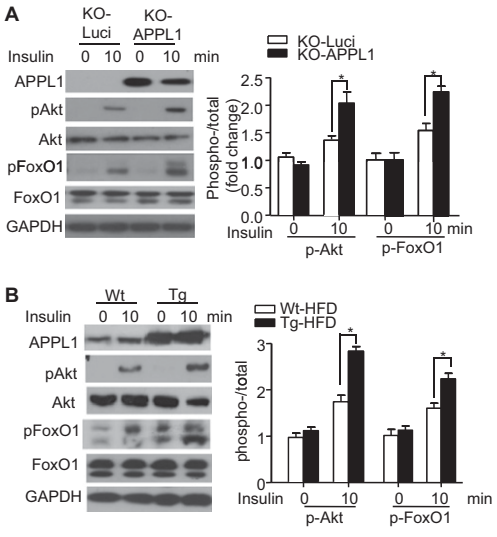

Fig. S7. APPL1 potentiates insulin-elicited phosphorylation of Akt and FoxO1 in pancreatic islets. (*A*) Islets from 20-wk-old male APPL1 KO mice were infected with recombinant adenovirus encoding luciferase (Luci) or APPL1 for 36 h, followed by starvation in a serum-free medium for 6 h and treatment with insulin (50 nM) for various time points as indicated. All cell lysates were subjected to Western blot analysis using antitotal or phospho-FoxO1 (Ser-256), antitotal or phospho-Akt (Ser-473), anti-APPL1 or anti-GAPDH antibody as a loading control. (*B*) Islets from 16-wk-old male APPL1 transgenic mice and WT littermates on HFD were subjected to the same analysis as in *A*. Bar chart on the *Right* represents the relative fold change of phosphorylation versus total as quantified by densitometry. $*P < 0.05$ ($n = 4$).

Table S1. Metabolic characterization of APPL1 KO and APPL1 transgenic mice

	STC		HFD	
20-wk-old male APPL1 KO and WT mice	WT	APPL1 KO	WT	APPL1 KO
Fasting glucose, mmol/L	3.3 ± 0.15	4.1 ± 0.30*	4.9 ± 0.40	6.0 ± 0.28*
Fasting insulin, ng/mL	0.25 ± 0.06	0.57 ± 0.079*	0.57 ± 0.069	1.035 ± 0.15*
Food intake, kcal/d	14.94 ± 0.33	14.97 ± 0.59	15.15 ± 0.39	14.94 ± 0.73
20-wk-old male APPL1 Tg and WT mice	WT	APPL1 Tg	WT	APPL1 Tg
Fasting glucose, mmol/L	4.3 ± 0.10	4.3 ± 0.14	6.48 ± 0.40	5.5 ± 0.18*
Fasting insulin, ng/mL	0.15 ± 0.03	0.12 ± 0.02	0.96 ± 0.0.18	0.36 ± 0.061*
Food intake, kcal/d	13.48 ± 0.77	13.26 ± 0.26	14.62 ± 0.69	15.01 ± 1.20
Body weight, g	30.78 ± 0.38	29.61 ± 1.26	39.16 ± 1.78	41.56 ± 2.66

*$P < 0.05$ versus WT control ($n = 8$ each group). HFD, high-fat diet; STC, standard chow.

Table S2. Primer sequences used for real-time PCR analysis

	Primer sequences	
Genes	Forward	Reverse
INS2	5′ TGGAGGCTCTCTACCTGGTG 3′	5′ TCTACAATGCCACGCTTCTG 3′
PDX-1	5′ GGTATAGCCGGAGAGATGC 3′	5′ CTGGTCCGTATTGGAACG 3′
GLUT2	5′ CTTGGTTCATGGTTGCTGAAT 3′	5′ GCAATGTACTGGAAGCAGAGG 3′
GCK	5′ ATCTTCTGTTCCACGGAGAGG 3′	5′ GATGTTAAGGATCTGCCTTCG 3′
STX1	5′ ATGGAGAAGGCTGATTCCAAC 3′	5′ CCATGAGAGAAGCATGAAGGA 3′
SNAP25	5′ GTGAGGAATTGGAAGACATGC 3′	5′ GCCTTGCTCTGGTACTTGACG 3′
VAMP2	5′ CCCACACACCAGGTTTTCTGT 3′	5′ GCAGGGGACACTGGGATAATA 3′
Munc18	5′ ATGAGGGCTGCCTATGAGGT 3′	5′ AGCGGGTTGGAGTAAGGATGT 3′
Rab3a	5′ GTTGACAGACGGCTTCTTCT 3′	5′ AGGGAGGAGTGGGACACATTT 3′
SNAPTO	5′ ACCTCGTCAACTCCCTTACCA 3′	5′ GGGCCTCATCCTCCTCAG A 3′